J Bone Miner Res. Author manuscript; available in PMC 2018 February 01.

Published in final edited form as:

J Bone Miner Res. 2017 February ; 32(2): 250–263. doi:10.1002/jbmr.2982.

Sex differences and growth-related adaptations in bone microarchitecture, geometry, density and strength from childhood to early adulthood: a mixed longitudinal HR-pQCT study

Leigh Gabel[1,2], **Heather M. Macdonald**[1,3], and **Heather A. McKay**[1,2,3,*]

[1]Department of Orthopaedics, University of British Columbia, Vancouver, Canada

[2]Centre for Hip Health and Mobility, Vancouver Coastal Health Research Institute, Vancouver, Canada

[3]Department of Family Practice, University of British Columbia, Vancouver, Canada

Abstract

Sex differences in bone strength and fracture risk are well-documented. However, we know little about bone strength accrual during growth and adaptations in bone microstructure, density and geometry that accompany gains in bone strength. Thus, our objectives are to 1) describe growth related adaptations in bone microarchitecture, geometry, density and strength at the distal tibia and radius in boys and girls; 2) compare differences in adaptations in bone microarchitecture, geometry, density and strength between boys and girls. We used HR-pQCT at the distal tibia (8% site) and radius (7% site) in 184 boys and 209 girls (9–20y at baseline). We aligned boys and girls on a common maturational landmark (age at peak height velocity; APHV) and fit a mixed effects model to these longitudinal data. Importantly, boys demonstrated 28–63% greater estimated bone strength across 12 years of longitudinal growth. Boys demonstrated 28–80% more porous cortices compared with girls at both sites across all biological ages, except at the radius at 9 years post-APHV. However, cortical density was similar between boys and girls at all ages at both sites, except at 9 years post-APHV at the tibia when girls' values were 2% greater than boys'. Boys demonstrated 13–48% greater cortical and total bone area across growth. Load-to-strength ratio was 26–27% lower in boys at all ages, indicating lower risk of distal forearm fracture compared with girls. Contrary to previous HR-pQCT studies that did not align boys and girls at the same biological age, we did not observe sex differences in Ct.BMD. Boys' superior bone size and strength compared with girls may confer them a protective advantage. However, boys' consistently more porous cortices may contribute to boys' higher fracture incidence during adolescence. Large prospective studies using HR-pQCT that target boys and girls who have sustained a fracture are needed to verify this.

[*]Corresponding Author: Heather McKay, PhD, Centre for Hip Health and Mobility, 7/F-2635 Laurel St, Vancouver, BC V5Z 1M9, heather.mckay@ubc.ca, Tel: 604.675.2585, Fax: 604.675.2576.

Disclosures: All authors state that they have no conflicts of interest.

Authors' roles: Study design and conduct: HMM and HAM. Data analysis: LG. Data interpretation: LG, HMM, HAM. Drafting, revising and approving final manuscript: LG, HMM, HAM. LG takes responsibility for the integrity of the data analysis.

Additional Supporting Information may be found in the online version of this article.

Keywords

HR-pQCT; bone accrual; bone strength; bone architecture; growth

Introduction

Bone strength, the 'bottom line' of fracture prevention, is influenced by many factors, including bone size, bone mineral density and the organization of bone microarchitecture.[1] However, the intricacies of bone microarchitectural adaptations as they relate to increased bone strength and fracture risk during growth are not well understood.

To date, few studies used high-resolution peripheral quantitative computed tomography (HR-pQCT) to evaluate sex differences in bone quality (i.e., bone microarchitecture, geometry and density) and bone strength accrual. Of these, most were cross-sectional or had only a short follow-up period.[2–5] However, these early studies were crucial as they began to shed light on changes in bone quality that occur during puberty. Two cross-sectional studies of children and adolescents aged 5–21 years observed a transiently thinner and less dense cortex in boys compared with girls at the radius[3], and at both radius and tibia[2] during mid-puberty. In our previous study, over a 2–3 year follow-up period we noted significantly more porous cortices in boys compared with girls as early as Tanner Stage 2 and 3.[4] We do not know whether these microarchitectural differences during puberty and deficits at the cortex, specifically, explain the high incidence of fractures in boys during periods of rapid pubertal growth.[6,7] Boys may be at a disadvantage during adolescent growth due to higher rates of bone turnover, longer duration of linear growth and greater peak height velocity compared with girls.[8,9] Evaluating bone strength and the parameters that underpin bone strength accrual prospectively over a longer time frame will further our understanding of factors that might contribute to elevated fracture risk during adolescence.

To assess sex differences in bone accrual during growth it is essential to account for the influence of maturational status, which varies considerably between children of the same chronological age.[10] Self-reported stage of maturation as per the method of Tanner is commonly used in cross-sectional and short-term prospective pediatric studies; however, boys and girls cannot be aligned on a similar maturational time point using this method.[11,12] In contrast, we[13] and others[14,15] compared bone accrual between boys and girls aligned on a common maturational landmark, age at peak height velocity (APHV). Commonly used as an indicator of somatic maturity in longitudinal studies,[10,16] APHV refers to the age when maximum linear growth in height occurs and generally occurs in boys and girls at a maturational time point when approximately 90% of adult stature has been achieved.[17] APHV can be determined either directly in longitudinal studies with adequate serial measures acquired around the period of maximal height velocity, or predicted in cross-sectional or short-term prospective studies using validated equations that incorporate common anthropometric measures such as height and sitting height.[18,19] APHV has not previously been used in pediatric bone studies that utilized HR-pQCT, to control for what could potentially be substantial differences in growth between and within sexes.

Thus, our objectives were to: 1) describe growth related adaptations in bone microarchitecture, geometry, density and strength at the distal tibia and radius in boys and girls, and 2) compare differences in growth related adaptations in bone microarchitecture, geometry, density and strength between boys and girls. We hypothesized that boys would demonstrate greater bone strength, geometry and cortical porosity, but lower cortical bone mineral density throughout growth compared with girls.

Methods

Study design

Participants were drawn from a mixed, longitudinal cohort of healthy girls (n=556) and boys (n=515) aged 8 to 12 years at study entry who comprised the University of British Columbia Healthy Bones Study III (HBSIII). The HBSIII cohort includes participants from three school-based studies (Table 1), described in detail elsewhere.[13] Briefly, we recruited participants from elementary schools in Vancouver and Richmond, British Columbia (BC), Canada, between 1999 and 2009. We recruited the first cohort (n=436), for HBS II[20–22] and the Bounce at the Bell study,[23] in the fall of 1999 and 2000, respectively, from grades 4, 5 and 6 classes in 14 schools in Richmond, BC. In February 2003, we recruited the second cohort (n=515) for the Action Schools! BC study[24] from grade 4 and 5 classes at 10 elementary schools in Vancouver and Richmond, BC. Participants in both cohorts attended annual follow-up measurements each spring after cessation of the school-based interventions. We combined the cohorts in 2006 because they employed nearly identical protocols. In the fall of 2009, we recruited a third cohort (n=120) from grade 4 and 5 classes in 5 schools in Vancouver and Richmond, BC. We recruited this cohort to study bone microarchitectural changes from pre-puberty through young adulthood using HR-pQCT, as this instrument was unavailable for our earlier studies.[4]

In the present analysis, we include HR-pQCT data from annual measurements conducted between May 2008 (first year of HR-pQCT measurements) and June 2012 in all three cohorts. In participants with HR-pQCT data (n=399) we acquired a median of 4 annual measurements at the distal tibia (interquartile range: 3 to 4) and a median of 3 annual measurements at the distal radius (interquartile range: 2 to 3). For the purpose of this analysis, we refer to data obtained at the first HR-pQCT measurement as baseline.

We obtained written informed consent from the parents or legal guardians, written assent from participants younger than 18 years of age and informed consent from participants 18 years of age and older. The University of British Columbia's Clinical Research Ethics Board approved the studies.

Anthropometry

We assessed standing and sitting height using standard stretch stature techniques.[25] We recorded measurements to the nearest millimeter using a wall-mounted stadiometer (Seca Model 242, Hanover, MD). We measured body mass to the nearest 0.1 kg using a calibrated electronic scale (Seca Model 840, Hanover, MD), with participants dressed in light clothing. We assessed limb length to the nearest 0.1cm as the distance from the distal edge of the

medial malleolus to the tibial plateau for the tibia and as the distance from the olecranon to the ulnar syloid process for the ulna. Trained reasearch assistants took all measurements in duplicate, unless differences were > 0.4cm or 0.2kg when they obtained a third measure. We used the mean of two values or the median of three for all analyses. In our laboratory, reproducibility (CV%) is <0.3% for measures of stature, <3.5% for tibia length and <1% for ulnar length (UBC Bone Health Research Group, unpublished data).

Maturity

We provide a detailed description of how we calculated APHV in Supplemental Document 1.[13,18] In brief, we fit an interpolating cubic spline to each participant's height velocity data. The magnitude of PHV was identified as growth per year (cm) that occurred at APHV. Due to missing and mistimed measurements surrounding APHV, we were only able to identify APHV using the cubic spline method in 198 participants (50% of cohort). For the remaining participants, we used the Moore equation[18] and anthropometric data from the measurement occasion closest to the expected APHV (approximately 11.6 years in girls and 13.5 years in boys) to estimate APHV.[18] For all participants we used APHV to calculate a continuous measure of biological maturity offset (in years) by subtracting APHV from chronological age at time of measurement (e.g., −1 year is equivalent to 1 year prior to attainment of APHV; +1 to one year after APHV).

For descriptive purposes, we also assessed maturity at each visit using the method of Tanner; self-reported pubic hair stage in boys and self-reported breast stage in girls.[26]

Health history, ethnicity and lifestyle

We determined health history and ethnicity using a questionnaire, completed by parents at baseline and by participants at subsequent annual visits. Based on questionnaire responses, we identified six participants who had conditions that prevented participation in regular physical activity and/or reported medical conditions known to influence bone metabolism (osteogenesis imperfecta, fetal alcohol syndrome, type 1 diabetes, leukemia, congenital heart defect). With these exclusions, we used data from 393 healthy participants (184 boys, 209 girls) for analysis.

We determined each participant's ethnicity based on their parents' response to questions regarding parents' and/or grandparents' place of birth and their self-identified ethnicity. We classified participants as "Asian" if both parents or three of four grandparents were born in Hong Kong, China, Japan, Taiwan, Philippines, Korea or India; "white" if both parents or three of four grandparents were born in North America or Europe; and "Other" if participant's parents were of other or mixed ethnicities.

Bone architecture, mineral density and strength

We assessed bone architecture, BMD and strength at the nondominant distal tibia and radius using HR-pQCT (XtremeCT; Scanco Medical AG, Brüttisellen, Switzerland), unless there was a previous fracture at the desired site, in which case the opposite limb was scanned.[4,27] In brief, we first performed a two-dimensional scout view over the joint line to define the anatomic reference line and used the same anatomical reference line to assess the same

relative site each year. We acquired a 9.02mm slice at the distal tibia (8% site; proximal to the tibial end plate) and distal radius (7% site; proximal to the medial edge of the distal radius).[28] The 8% and 7% site at the distal tibia and radius, respectively, ensured that scans would not include the growth plate in most children and that the same relative regions could be scanned at follow-up (Figure 1).[28] We scanned all participants using manufacturer's standard protocol of 60-kVp effective energy, 900 KA, matrix size of 1536 1536, and 100-ms integration time to acquire 110 slices at an 82-μm nominal isotropic resolution. The first three and last three slices were excluded from the analysis as per manufacturer's protocol. The effective dose equivalent for the scan is less than 3 μSv per measurement; measurement time was 2.8 min. We conducted daily quality control procedures to assess density fluctuation and weekly procedures to standardize geometry using a calibration phantom provided by the manufacturer.

A single qualified technician evaluated all HR-pQCT for motion artifacts and analyzed all scans as per manufacturer's standard protocol.[29,30] We excluded 1 tibia scan and 33 radius scans (3%) due to motion artifact >3 (on a scale from 1 to 5); [31]exclusions were fewer compared with other studies of the radius that used HR-pQCT in adolescent populations.[3,32] Briefly, a semi-automated segmentation method was used to trace the periosteal surface of the tibia and radius. Following this, a threshold-based algorithm separated the cortical and trabecular bone. We report standard morphological measures including: total BMD (Tt.BMD, mg/cm^3), trabecular number (Tb.N, 1/mm), thickness (Tb.Th, mm), separation (Tb.Sp, mm), bone volume ratio (BV/TV). Additionally we use an automated segmentation algorithm to separate trabecular and cortical bone[33,34] to determine: total bone cross-sectional area (Tt.Ar, mm^2), cortical BMD (Ct.BMD, mg/cm^3), porosity (Ct.Po, %), and thickness (Ct.Th, mm). Finally, we applied a validated finite element (FE) analysis to HR-pQCT images to estimate bone strength. We simulated uniaxial compression up to 1% strain using a single homogenous tissue modulus of 6829 MPa and a Poisson ratio of 0.3.[35] FE outcomes were failure load (F.Load, N) and ultimate stress (U.Stress). We also calculated load-to-strength ratio (distal radius only) as the a ratio of estimated fall load applied to the outstretched hand after a fall from standing height (simulation model that includes participant's height):[36]

$$\textbf{Fall Load (N)} = \frac{\mathbf{670}\sqrt{\mathbf{2} * \mathbf{9.81} * \frac{\boldsymbol{height}}{\mathbf{2}}}}{\mathbf{10}} \text{ and FE- based F. Load.}$$

Statistical analysis

We performed all analyses using STATA, Version 12.1 (StataCorp, College Station, TX) and considered P-values <0.05 statistically significant. Prior to modeling our data, we examined scatter plots generated for bone microarchitecture and strength against maturity offset for each participant. We fit general linear mixed models (also called random coefficients regression models or multilevel models) to compare annual rate of change in bone parameters between girls and boys. Maturity offset was centered at 0, a maturational landmark used previously in pediatric studies.[10] All models were estimated using maximum likelihood estimation, as there was only a 0.3% downward bias in the random

intercept variance compared with restricted maximum likelihood estimation (assessed using Ct.Ar at the distal tibia as the outcome).

We used the following process to determine the best fit model for all variables. First, we conducted an empty means random intercept model to determine the amount of variance attributed to between-person and within-person differences. Next, we assessed a fixed linear time, with maturity offset (APHV) as the time variable, random intercept model, followed by a random linear time model. We followed these models with fixed quadratic and cubic time models. Wald test p-values were used to determine significance of individual fixed effects and the maximum log likelihood (−2*log likelihood (LL)) statistics were used to determine significance of random effects variances and covariances between nested models given the difference in model degrees of freedom. We determined the best fit unconditional growth model by the largest reduction in the deviance test (−2LL) and parsimony of the model (Akaike and Bayesian information criterion (AIC and BIC) values). We examined change in pseudo R^2 with addition of each fixed polynomial time (as computed from the square of the correlation between the observed bone variable and the outcomes predicted by the fixed effects) to assess potential for overfitting of the model. If a negligible change in pseudo R^2 (<1%) suggested the presence of overfitting, we used the previous model. We then examined the effect of sex and ethnicity on the intercept and maturity effects. We provide an example of a mixed model below.

Random linear, fixed quadratic maturity model, including fixed effect of sex and ethnicity predicting intercept, and sex predicting linear and quadratic maturity slope

$$Level\ 1{:}\ y_{ti}=\beta_{0i}+\beta_{1i}MO_{ti}+\beta_{2i}MO_t{}^2+\varepsilon_{ti}$$
$$Level\ 2{:}\ Intercept{:}\ \beta_{0i}=\gamma_{00}+\gamma_{01}\,Boys_i+\gamma_{02}\,Ethnicity_i+\mu_{0i}$$
$$Linear\ time{:}\ \beta_{1i}=\gamma_{10}+\gamma_{11}\,Boys_i+\mu_{1i}$$
$$Quadratic\ time{:}\ \beta_{2i}=\gamma_{20}+\gamma_{21}\,Boys_i$$
$$Composite{:}\ y_{ti}=[\gamma_{00}+\gamma_{10}\,MO_{ti}+\gamma_{20}\,MO_{ti}{}^2+\gamma_{01}\,Boys_i+\gamma_{11}\,MO_{ti}*Boys_i+\gamma_{21}\,MO_{ti}{}^2*Boys_i+\gamma_{02}\,Ethnicity_i]+[\mu_{0i}+\mu_{1i}MO_{ti}$$

MO is maturity offset (centered at 0, APHV); Boys = 0, girl; 1, boy

Ethnicity= 0, Asian; 1, white; 2, other

where y_{ti} is the bone parameter on measurement occasion t in the i^{th} individual, $(\mu_{0i}, \mu_{1i} \sim N(0,\Sigma)$ is the vector of random effects for the i^{th} individual and $\varepsilon_{ij} \sim N(0,\sigma^2)$ is the within-subject residual error.

Thus, the intercepts γ_{00}, $\gamma_{01}Boys_i$ *and* $\gamma_{02}Ethnicity_i$ represent the mean value of the bone parameter and the fixed effect of sex and ethnicity on the mean intercept of the bone parameter when maturity offset is zero, respectively, while μ_{0i} is the person-specific deviation from the mean intercept. The slopes γ_{10} and $\gamma_{11}Boys$ represent the fixed linear effect of maturity and the fixed effect of sex on linear maturity at APHV, respectively, while $\mu_{1i}$is the person-specific deviation from the fixed linear effect of time. The slopes γ_{20} and $\gamma_{21}Boys$ represent the fixed quadratic effect of maturity and the fixed effect of sex on quadratic maturity, respectively. We checked model adequacy graphically using plots of transformed residuals.[37] Diagnostic checking of fitted models revealed some serial

correlation in the residuals; however, attempting to incorporate a serial correlation component into the model led to problems with model convergence, an issue identified by others.[37] Models that included serial correlation and only a random intercept yielded similar results to the random coefficients only model. We calculated adjusted means and estimated sex differences in bone parameters at each biological age using the margins command in Stata and a Bonferroni adjustment to account for multiple comparisons. Accordingly, the level of statistical significance was set to $p<0.0042$ ($p<0.05$ divided by 12) for sex differences.

Results

Descriptive characteristics

We provide participant characteristics and bone parameters at first HR-pQCT measurement in Table 2. There were 1240 total observations at the distal tibia and 915 total observations at the distal radius (Table 3). We deliberately did not compare parameters between boys and girls at baseline as their chronological age and maturity varied significantly. Alternatively, we compared differences in all parameters between boys and girls at the same approximate biological time point (APHV). We provide predicted model parameters and growth curves at the tibia (Table 4, Figure 2) and at the radius (Table 5, Figure 3). We compare sex differences in bone parameters at each biological age across 12 years (Figure 4, Figure 5 and Supplemental Tables 1 and 2). Due to few measurements at biological ages before 2 years prior to APHV in girls (n=3) and after 9 years post-APHV in boys (n=6), we limited our range of between-sex comparisons from 2 years prior to APHV to 9 years post-APHV.

General growth patterns at the distal tibia and radius

Based on growth curves for HR-pQCT outcomes (Figures 2 and 3), boys and girls demonstrated net gains in Tb.Th, Ct.Th, Ct.Ar, Tt.Ar, Ct.BMD, Tt.BMD, F.Load and U.Stress and net losses in Ct.Po across 12 years of adolescent growth at both the distal tibia and radius. Trajectories for most parameters at both sites indicated increases during adolescence in boys and girls. However, curves for Ct.BMD, Tt.BMD and Ct.Th at the distal radius suggest transient decreases around APHV. Conversely, curves for Ct.Po suggest a transient increase around APHV at both sites in boys and at the radius in girls, prior to declining after APHV.

The magnitude of change in bone parameters during adolescence was similar between boys and girls at both sites (percent change provided in Supplemental Tables 1 and 2). However, trabecular microarchitecture parameters demonstrated some site- and sex-specific variation with maturation. At the distal tibia, Tb.N remained relatively unchanged across adolescence (1% and −5% change in boys and girls, respectively; between biological age −2 to +9). However, at the radius, Tb.N decreased in boys (−9%) and girls (−13%) between biological age −2 to +9. Similarly, Tb.Sp demonstrated little change at the distal tibia (−5% and 3% change in boys and girls, respectively), but increased at the distal radius (7% and 17% in boys and girls, respectively). Boys demonstrated an approximately 20% increase in BV/TV from biological age −2 to +9 at both sites. Girls' BV/TV increased by 10% at the distal tibia and remained relatively stable at the distal radius.

Comparisons of model estimates of bone parameters between boys and girls Tibia

At the distal tibia, boys compared with girls, demonstrated significantly greater Ct.Th, Ct.Po, Ct.Ar, Tt.Ar, and F.Load at equivalent maturational time points across growth (Figure 4). Values were significantly greater for boys from 1 year prior to APHV onwards for BV/TV; 1 year post-APHV and beyond for Tb.N and U.Stress; and beyond 1 year post-APHV for Tt.BMD. Boys demonstrated significantly greater Tb.Th compared with girls prior to APHV and no differences thereafter. Tb.Sp was significantly lower in boys compared with girls at all biological ages post-APHV. Ct.BMD was similar between boys and girls at all biological ages except at 9 years post-APHV when girls' values were greater than boys'.

Radius

At the distal radius, boys demonstrated significantly greater Ct.Ar, Tt.Ar and F.Load across 12 years of adolescent growth compared with girls (Figure 5). Load-to-strength ratio was significantly lower in boys compared with girls at all biological ages (Figure 6). Bone parameters were significantly greater in boys from 1 year prior to APHV onward for Tb.Th; from APHV onward for BV/TV and Ct.Th; and greater post-APHV for U.Stress and Tt.BMD. Tb.N was significantly greater in boys from 3–5 years post-APHV. Tb.Sp was significantly lower in boys compared with girls from 2 to 8 years post-APHV. Ct.Po was greater in boys compared with girls at all biological ages except at 9 years post-APHV, when boys' Ct.Po was the same as girls'. There were no significant sex differences in Ct.BMD at any biological age.

Discussion

In this study we used longitudinal data and multilevel modeling approaches to demonstrate sex differences in bone microarchitecture, geometry, density and strength at the distal tibia and radius across adolescence and into young adulthood. Longitudinal data capture nuanced adaptations of bone over time and overcome the many limitations of cross-sectional data. Despite this – few long term prospective studies have been conducted, most likely due to the time and labour intensive nature of this type of investigation. We aligned boys and girls on a common maturational landmark (APHV) to more clearly characterize changes in 3-dimensional aspects of bone quality across adolescence. Our study highlights similarities in the magnitude of bone accrual at the distal tibia compared with the distal radius, and sex differences therein, despite substantially different loading environments. Further, we report significant sex differences in bone microarchitecture, geometry and strength at both sites across growth. We observed substantially more porous cortices in boys in the years around peak linear growth, which may contribute to greater skeletal fragility in boys during adolescence.

Trabecular microarchitecture

Trabecular bone density may increase by way of gains in material density or trabecular number, or through thickening of trabeculae. Our finding of increased Tb.Th throughout growth is consistent with previous work.[4,39] That is, increases in the amount of trabecular bone (expressed as BV/TV) during growth are underpinned by thickening of trabeculae, with

little to no change in Tb.N or Tb.Sp. Thickening of trabeculae during growth has been attributed to remodeling with a positive balance, such that more bone is added during each remodeling cycle than was previously resorbed.[38,39] Although a slow process, in theory, trabeculae thicken with each subsequent remodeling cycle.

We also observed site-and sex-specific differences in trabecular volume across adolescence. Boys in our study and others'[2–4] demonstrated consistent increases in BV/TV throughout growth at both distal sites. However, BV/TV at the distal radius did not change significantly in girls. Thus, given similar Tb.N and Tb.Sp, the observed sex difference in BV/TV at the radius is driven by thicker trabeculae in boys. The mechanism underlying the sex-specificity of BV/TV is not entirely clear. Although we did not assess hormonal markers in our study, Kirmani and colleagues assessed growth and reproductive hormonal markers in their cross-sectional study of bone architecture at the distal radius in 127 participants aged 6–21 years. They noted a significant relationship between BV/TV and testosterone in boys, but no such relationship with any hormones in girls. The authors speculated that girls' BV/TV at the radius is programmed early in life.[3] Finally, we observed comparable Tb.Th in boys and girls at the distal tibia, suggesting similar adaptations to the greater mechanical loads experienced at this weight-bearing site.

Cortical microarchitecture, bone geometry and estimated bone strength

We noted consistently larger bone size in boys compared with girls at the distal tibia and radius. Similar findings were reported in previous studies that assessed bone using pQCT and HR-pQCT and that accounted for differences in maturational status using the method of Tanner or APHV.[2,4,13,40,41] Even small differences in bone size confer substantial increases in resistance to compressive and bending forces.[42] Thus, it is not surprising that boys also demonstrated consistently greater bone strength compared with girls across adolescence and into young adulthood at both skeletal sites. At the distal radius, greater bone strength in boys also contributed to a lower load-to-strength ratio, an indicator of fracture risk,[36] compared with girls.

Adaptations at the cortex, specifically changes in porosity during peak growth, also contribute to bone strength. The exponential relationship between porosity and strength dictates that small decreases in porosity may result in large gains in bone strength.[43] We found that adolescent growth is characterized by significant decreases in Ct.Po and concurrent increases in Ct.Th. Importantly, our data and that of others[3,4] show a transient period of increased porosity at the cortex during periods of rapid growth at both skeletal sites. Moreover, we confirm that boys demonstrate greater Ct.Po compared with girls at both bone sites, a finding we previously noted over a shorter time period.[4] This is likely explained by boys' longer period of adolescent growth and greater linear growth velocity.[8,44]

Our data also suggest a transient decrease in Ct.Th and Ct.BMD around peak growth at the distal radius; also observed by others.[2,3] We did not observe thickening of the distal radius cortex until 1 year post-APHV (approximately 12.6 years and 14.5 years in girls and boys, respectively). This is consistent with results of a cross-sectional study by Rauch and colleagues who did not observe increases in Ct.Th at the distal radius (by pQCT) until after

Tanner Stage 4, or approximately 13 years and 15 years of age in girls and boys, respectively.[45] The authors contend that distal radius Ct.Th remains relatively stable until late puberty, as endosteal apposition is unable to keep pace with the rapid periosteal resorption that dominates the process of metaphyseal inwaisting during periods of rapid longitudinal growth.[45] The lag in Ct.Th we observed at the radius may contribute to increased forearm fracture risk. However, this finding is in contrast to that observed at the distal tibia in the current study and in our previous study at the tibial shaft,[13] where thickening of the cortex was evident throughout growth. The substantially different forces experienced at the non weight-bearing radius compared with the weight-bearing tibia may contribute to site-specific differences in growth-related adaptations.

A heightened period of bone fragility during the pubertal growth spurt is thought to be a direct result of increased calcium demands, resulting in higher rates of intracortical bone turnover and increased porosity due to incomplete consolidation of bone.[9] Alternatively, trabecular coalescence may be incomplete.[46] Longitudinal growth proceeds by producing new trabeculae at the growth plate, which eventually coalesce into the cortical shell. That is, the further bone is from the growth plate, the greater number of loading cycles it experiences. [46] Newly formed bone requires time (and probably mechanical stimulus) to coalesce – luxuries not available during the rapid adolescent growth spurt. The underlying mechanism for the sex-difference in porosity aligns well with the theory by Tanck,[46] whereby more rapid growth in boys results in more immature bone at metaphyses compared with girls. In our study, Ct.Po was the only bone parameter that was deficit in boys compared with girls in the years around peak linear growth. Thus, while we cannot rule out other determinants, our findings support the hypothesis that increased Ct.Po during peak growth may contribute to the higher incidence of forearm fractures rates in boys during this time.[9]

It is interesting that sex differences in Ct.Po didn't manifest in our estimates of bone strength and estimated fracture risk at the distal radius. Specifically, boys, in comparison with girls, demonstrated greater estimated bone strength and lower fracture risk despite greater porosity. This is consistent with a recent cohort study in which adult forearm fracture cases exhibited significantly more porous cortices at the distal radius (by HR-pQCT) compared with non-fracture controls, despite similar estimates of bone strength.[47] There are several possible explanations for this discrepancy. First, greater porosity in boys may be somewhat compensated for by their substantially larger bones compared with girls. Second, porosity may be localized to specific regions of the cortex that contribute less to mechanical competence. Porosity varies significantly across regions of the cortex,[48] and porosity on the endocortical surface experiences lower mechanical stress compared with porosity localized to the periosteal surface.[43] Thus, regional analyses within the same bony compartment may help clarify the porosity-strength relationship during growth, in future.[48] Third, the resolution of HR-pQCT may be insufficient to accurately assess porosity at the distal end of the radius where the cortical shell is quite thin; thereby, systemically underestimating cortical porosity,[49] an explanation offered by Vilayphiou and colleagues. [50] Finally, it is possible that FE estimates of bone strength do not capture changes in porosity that contribute to transient increases in bone fragility. Forearm fractures are a consequence of compressive

and bending forces.[51] Therefore, FE-estimates of bone strength need to incorporate stress associated with bending in addition to compressive loads.[4]

The transient decreases in Ct.BMD and Tt.BMD observed at the distal radius surrounding peak growth may reflect increased porosity during this time. However, despite significant sex differences in porosity and contrary to our previous studies,[4,5] we did not observe denser cortices in girls compared with boys at the distal tibia or radius (with the exception of greater Ct.BMD in girls 9 years post-APHV). Although the finding of similar Ct.BMD despite greater cortical porosity among boys suggests that boys may compensate for larger cortical pores with greater cortical material mineral density, we are unable to confirm this using currently available imaging methods. The discrepancy regarding sex differences in Ct.BMD may be partially explained by methodological differences in maturity assessment, as for our previous studies we relied on self-reported stage of sexual maturation.[26] While feasible for use in cross-sectional and short-term prospective studies, comparisons between sexes at the same Tanner stage are confounded by differences in the timing of growth relative to development of secondary sex characteristics. Specifically, the majority of girls attain PHV by Tanner stage 3, whereas most boys do not reach PHV until Tanner stage 4.[11,12]

In our previous study,[4] when we compared girls and boys at the same Tanner stage, we noted significantly greater Ct.BMD in girls compared with boys at peri- (Tanner stage 4) and post-puberty (Tanner stage 5) at both skeletal sites. However, girls would have been more mature than boys at these Tanner Stages, on average, based on APHV. If we account for this by comparing values for girls at Tanner Stage 4 with boys at Tanner Stage 5, Ct.BMD values are virtually identical at the distal tibia (813 ± 100.8 vs. 815.5 ± 68.6) and radius (835.3 ± 52.1 vs. 821.7 ± 42.7). This premise held true when we visually examined cross-sectional HR-pQCT values at the distal radius as per Kirmani et al[3] and at the radius and tibia as per Wang and colleagues.[2] If one supports this contention, it also explains sex differences reported at the distal radius using pQCT.[41] Thus, aligning by APHV may more adequately control for differences in body size, and the notion that girls have greater Ct.BMD at distal sites in later maturity may be an artifact of the method used to control for maturity.

Our study has several limitations. First, as in any repeated measures study of growing bone, it is not possible to reassess the exact same bone cross section over time. Long bone growth is both complex and disproportionate; at the tibia, 57% of longitudinal growth occurs at the proximal metaphysis and 43% occurs at the distal metaphysis.[52] Therefore, we used a standard anatomical landmark to identify the same relative site along the length of the tibia and radius at each measurement in every child. Second, based on differences in maturational timing between boys and girls at the same chronological age, many of the girls in our study approached APHV at baseline. Thus, we were only able to compare boys and girls up to 2 years prior to APHV. Third, we note that our ethnically diverse sample limits the generalizability of our findings outside the Metro Vancouver area, where visible minority groups represent 47% of the population.[53] While we did not specifically aim to examine ethnic differences in bone accrual in the present study, we recognized the need to control for known differences in the timing and tempo of maturation between ethnic groups. For example, Asian participants in our cohort attained APHV approximately 7 months prior to

their white peers. We accounted for this by aligning participants on APHV. Fourth, we were unable to align bone data to fracture occurrence. Although we explored the relationship between bone microarchitecture and forearm fractures in a separate cohort,[32] prospective studies are warranted to clarify the influence of bone microarchitecture on fracture risk. Finally, the minimal change in Tb.N and Tb.Sp observed across growth (1–17%) was in some cases comparable with relatively high least significant change values (LSC % ~15–20%) reported previously.[54] Thus, the observed decrease in Tb.N across growth at the distal radius, may represent a measurement artifact in cases where the resolution of HR-pQCT was unable to capture thin trabeculae.

Our study was uniquely positioned to examine sex differences in longitudinal patterns of growth-related adaptations in bone microarchitecture, geometry, density and strength across adolescent growth, with boys and girls aligned on a common measure of somatic maturity. We note boys' superior bone size and strength compared with girls' across maturity. Contrary to previous HR-pQCT studies that compared boys and girls according to self-reported stage of sexual maturation, we did not observe sex differences in Ct.BMD during peak growth. We suggest that compared with girls, boys' substantially more porous cortices throughout growth may partially explain their greater skeletal fragility during the pubertal growth spurt. This hypothesis would benefit from prospective studies comparing microarchitectural parameters between boys and maturity-matched female peers who have sustained a fracture.

Supplementary Material

Refer to Web version on PubMed Central for supplementary material.

Acknowledgments

We gratefully acknowledge the HBSIII participants, their families and the support from principals and teachers at participating schools in the Richmond and Vancouver School Districts. We also acknowledge the dedication of the HBSIII research teams, the efforts of our research coordinator, Douglas Race, and the supervision of imaging acquisition and processing from Dr. Danmei Liu and Dr. Mikko Maatta (Centre for Hip Health and Mobility, Vancouver Coastal Research Institute). We received funding from the Canadian Institutes of Health Research (CIHR; MOP-84575) to support this work. HMc was supported by the British Columbia Health Research Foundation (2400–2 and 10898–2) and the Michael Smith Foundation for Health Research (MSFHR). LG was supported by a CIHR Doctoral Research Award.

References

1. Järvinen TL, Sievänen H, Jokihaara J, Einhorn TA. Revival of Bone Strength: The Bottom Line. J Bone Miner Res. 2005; 20(5):717–720. [PubMed: 15824843]
2. Wang Q, Wang X-F, Iuliano-Burns S, Ghasem-Zadeh A, Zebaze R, Seeman E. Rapid growth produces transient cortical weakness: a risk factor for metaphyseal fractures during puberty. J Bone Miner Res. 2010; 25(7):1521–1526. [PubMed: 20200962]
3. Kirmani S, Christen D, van Lenthe GH, et al. Bone structure at the distal radius during adolescent growth. J Bone Miner Res. 2009; 24(6):1033–1042. [PubMed: 19113916]
4. Nishiyama KK, Macdonald HM, Moore SA, Fung T, Boyd SK, McKay HA. Cortical porosity is higher in boys compared with girls at the distal radius and distal tibia during pubertal growth: An HR-pQCT study. J Bone Miner Res. 2012; 27(2):273–282. [PubMed: 22028110]

5. Burrows M, Liu D, Moore S, McKay H. Bone microstructure at the distal tibia provides a strength advantage to males in late puberty: an HR-pQCT study. J Bone Miner Res. 2010; 25(6):1423–1432. [PubMed: 19874197]
6. Cooper C, Dennison EM, Leufkens HGM, Bishop N, van Staa TP. Epidemiology of childhood fractures in Britain: a study using the general practice research database. J Bone Miner Res. 2004; 19(12):1976–1981. [PubMed: 15537440]
7. Randsborg P-H, Gulbrandsen P, Šaltytė Benth J, et al. Fractures in Children: Epidemiology and Activity-Specific Fracture Rates. J Bone Joint Surg Am. 2013; 95(7):e421.
8. Bailey DA, Wedge JH, McCulloch RG, Martin AD, Bernhardson SC. Epidemiology of fractures of the distal end of the radius in children as associated with growth. J Bone Joint Surg Am. 1989; 71(8):1225–1231. [PubMed: 2777851]
9. Parfitt AM. The two faces of growth: benefits and risks to bone integrity. Osteoporos Int. 1994; 4(6): 382–398. [PubMed: 7696836]
10. Baxter-Jones ADG, Eisenmann JC, Sherar LB. Controlling for maturation in pediatric exercise science. Ped Exerc Sci. 2005; 17:18–30.
11. Sherar LB, Baxter-Jones ADG, Mirwald RL. Limitations to the use of secondary sex characteristics for gender comparisons. Ann Hum Biol. 2004; 31(5):586–593. [PubMed: 15739387]
12. Granados A, Gebremariam A, Lee JM. Relationship Between Timing of Peak Height Velocity and Pubertal Staging in Boys and Girls. JCRPE. 2015; 7(3):235–237. [PubMed: 26831559]
13. Gabel L, Nettlefold L, Brasher PM, et al. Reexamining the Surfaces of Bone in Boys and Girls During Adolescent Growth: A 12-Year Mixed Longitudinal pQCT Study. J Bone Miner Res. 2015; 30(12):2158–2167. [PubMed: 26058373]
14. Baxter-Jones ADG, Mirwald RL, McKay HA, Bailey DA. A longitudinal analysis of sex differences in bone mineral accrual in healthy 8–19-year-old boys and girls. Ann Hum Biol. 2003; 30(2):160–175. [PubMed: 12637192]
15. Bailey DA, McKay HA, Mirwald RL, Crocker PR, Faulkner RA. A six-year longitudinal study of the relationship of physical activity to bone mineral accrual in growing children: the University of Saskatchewan bone mineral accrual study. J Bone Miner Res. 1999; 14(10):1672–1679. [PubMed: 10491214]
16. Malina, RM., Bouchard, C., Bar-Or, O. Human Kinetics. 2. Growth, maturation, and physical activity.
17. Bailey DA. The Saskatchewan Pediatric Bone Mineral Accrual Study: bone mineral acquisition during the growing years. Int J Sports Med. 1997; 18(Suppl 3):S191–4. [PubMed: 9272847]
18. Moore SA, McKay HA, Macdonald H, et al. Enhancing a Somatic Maturity Prediction Model. Med Sci Sports Exerc. 2015; 47(8):1755–1764. [PubMed: 25423445]
19. Mirwald RL, Baxter-Jones ADG, Bailey DA, Beunen GP. An assessment of maturity from anthropometric measurements. Med Sci Sports Exerc. 2002; 34(4):689–694. [PubMed: 11932580]
20. MacKelvie KJ, McKay HA, Khan KM, Crocker PR. A school-based exercise intervention augments bone mineral accrual in early pubertal girls. J Pediatr. 2001; 139(4):501–508. [PubMed: 11598595]
21. MacKelvie KJ, Petit MA, Khan KM, Beck TJ, McKay HA. Bone mass and structure are enhanced following a 2-year randomized controlled trial of exercise in prepubertal boys. Bone. 2004; 34(4): 755–764. [PubMed: 15050908]
22. MacKelvie KJ, McKay HA, Petit MA, Moran O, Khan KM. Bone mineral response to a 7-month randomized controlled, school-based jumping intervention in 121 prepubertal boys: associations with ethnicity and body mass index. J Bone Miner Res. 2002; 17(5):834–844. [PubMed: 12009014]
23. McKay HA, MacLean L, Petit M, et al. “Bounce at the Bell”: a novel program of short bouts of exercise improves proximal femur bone mass in early pubertal children. B J Sports Med. 2005; 39(8):521–526.
24. Macdonald HM, Kontulainen SA, Khan KM, McKay HA. Is a school-based physical activity intervention effective for increasing tibial bone strength in boys and girls? J Bone Miner Res. 2007; 22(3):434–446. [PubMed: 17181400]

25. Ross, W., Marfell-Jones, M. Kinanthropometry. In: Green, H., editor. Physiological testing of the high performance athlete. Champaign, IL: Human Kinetics; 1991.
26. Tanner, JM. Foetus into man. Cambridge: Harvard Press; 1978.
27. Gabel L, McKay HA, Nettlefold L, Race D, Macdonald HM. Bone architecture and strength in the growing skeleton: the role of sedentary time. Med Sci Sports Exerc. 2015; 47(2):363–372. [PubMed: 24983338]
28. Burrows M, Liu D, Perdios A, Moore S, Mulpuri K, McKay H. Assessing bone microstructure at the distal radius in children and adolescents using HR-pQCT: a methodological pilot study. J Clin Densitom. 2010; 13(4):451–455. [PubMed: 20663697]
29. Laib A, Barou O, Vico L, Lafage-Proust MH, Alexandre C, Rügsegger P. 3D micro-computed tomography of trabecular and cortical bone architecture with application to a rat model of immobilisation osteoporosis. Med Biol Eng Comput. 2000; 38(3):326–332. [PubMed: 10912350]
30. MacNeil JA, Boyd SK. Accuracy of high-resolution peripheral quantitative computed tomography for measurement of bone quality. Med Eng Phys. 2007; 29(10):1096–1105. [PubMed: 17229586]
31. Pauchard Y, Liphardt A-M, Macdonald HM, Hanley DA, Boyd SK. Quality control for bone quality parameters affected by subject motion in high-resolution peripheral quantitative computed tomography. Bone. 2012; 50(6):1304–1310. [PubMed: 22445540]
32. Määttä M, Macdonald HM, Mulpuri K, McKay HA. Deficits in distal radius bone strength, density and microstructure are associated with forearm fractures in girls: an HR-pQCT study. Osteoporos Int. 2015; 26(3):1163–1174. [PubMed: 25572041]
33. Buie HR, Campbell GM, Klinck RJ, MacNeil JA, Boyd SK. Automatic segmentation of cortical and trabecular compartments based on a dual threshold technique for in vivo micro-CT bone analysis. Bone. 2007; 41(4):505–515. [PubMed: 17693147]
34. Nishiyama KK, Macdonald HM, Buie HR, Hanley DA, Boyd SK. Postmenopausal women with osteopenia have higher cortical porosity and thinner cortices at the distal radius and tibia than women with normal aBMD: an in vivo HR-pQCT study. J Bone Miner Res. 2010; 25(4):882–890. [PubMed: 19839766]
35. MacNeil JA, Boyd SK. Bone strength at the distal radius can be estimated from high-resolution peripheral quantitative computed tomography and the finite element method. Bone. 2008; 42(6): 1203–1213. [PubMed: 18358799]
36. Chiu J, Robinovitch SN. Prediction of upper extremity impact forces during falls on the outstretched hand. Journal of biomechanics. 1998; 31(12):1169–1176. [PubMed: 9882050]
37. Verbeke, G., Molenberghs, G. Linear mixed models for longitudinal data. New York: Springer-Verlag; 2000.
38. Rauch F. Bone accrual in children: adding substance to surfaces. Pediatrics. 2007; 119(Suppl 2):S137–40. [PubMed: 17332233]
39. Parfitt AM, Travers R, Rauch F, Glorieux FH. Structural and cellular changes during bone growth in healthy children. Bone. 2000; 27(4):487–494. [PubMed: 11033443]
40. Kontulainen SA, Macdonald HM, Khan KM, McKay HA. Examining bone surfaces across puberty: a 20-month pQCT trial. J Bone Miner Res. 2005; 20(7):1202–1207. [PubMed: 15940373]
41. Neu CM, Manz F, Rauch F, Merkel A, Schoenau E. Bone densities and bone size at the distal radius in healthy children and adolescents: a study using peripheral quantitative computed tomography. Bone. 2001; 28(2):227–232. [PubMed: 11182383]
42. Ruff C, Holt B, Trinkaus E. Who's afraid of the big bad Wolff?: 'Wolff's law' and bone functional adaptation. Am J Phys Anthropol. 2006; 129(4):484–498. [PubMed: 16425178]
43. Turner CH. Biomechanics of bone: determinants of skeletal fragility and bone quality. Osteoporos Int. 2002; 13(2):97–104. [PubMed: 11905527]
44. Tanner JM, Whitehouse RH, Marubini E, Resele LF. The adolescent growth spurt of boys and girls of the Harpenden growth study. Ann Hum Biol. 1976; 3(2):109–126. [PubMed: 1275435]
45. Rauch F, Neu C, Manz F, Schoenau E. The development of metaphyseal cortex--implications for distal radius fractures during growth. J Bone Miner Res. 2001; 16(8):1547–1555. [PubMed: 11499878]

46. Tanck E, Hannink G, Ruimerman R, Buma P, Burger EH, Huiskes R. Cortical bone development under the growth plate is regulated by mechanical load transfer. J Anat. 2006; 208(1):73–79. [PubMed: 16420380]
47. Patsch JM, Burghardt AJ, Yap SP, Baum T, Schwartz AV, Joseph GB, Link TM. Increased cortical porosity in type 2 diabetic postmenopausal women with fragility fractures. J Bone Miner Res. 2013; 28(2):313–324. [PubMed: 22991256]
48. Kazakia GJ, Nirody JA, Bernstein G, Sode M, Burghardt AJ, Majumdar S. Age- and gender-related differences in cortical geometry and microstructure: Improved sensitivity by regional analysis. Bone. 2013; 52(2):623–631. [PubMed: 23142360]
49. Jorgenson BL, Buie HR, McErlain DD, Sandino C, Boyd SK. A comparison of methods for in vivo assessment of cortical porosity in the human appendicular skeleton. Bone. 2015; 73:167–175. [PubMed: 25540917]
50. Vilayphiou N, Boutroy S, Sornay-Rendu E, Van Rietbergen B, Chapurlat R. Age-related changes in bone strength from HR-pQCT derived microarchitectural parameters with an emphasis on the role of cortical porosity. Bone. 2016; 83(C):233–240. [PubMed: 26525593]
51. Einhorn TA. Bone strength: the bottom line. Calcif Tissue Int. 1992; 51(5):333–339. [PubMed: 1458335]
52. Anderson M, Green WT, Messner MB. Growth and predictions of growth in the lower extremities. Clin Orthop Relat Res. 1963; (45-A):1–14.
53. Statistics Canada. Table 2 Visible minority population and top three visible minority groups, selected census metropolitan areas, Canada. Ottawa, ON: Statistics Canada; 2011.
54. Kawalilak CE, Johnston JD, Olszynski WP, Kontulainen SA. Least significant changes and monitoring time intervals for high-resolution pQCT-derived bone outcomes in postmenopausal women. J Musculoskelet Neuronal Interact. 2015; 15(2):190–196. [PubMed: 26032212]

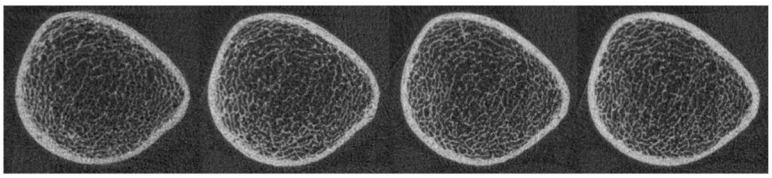

Figure 1.
Representative HR-pQCT images at the distal tibia from a single participant across 4 years acquired at 11 (far left), 12, 13 and 14 (far right) years of age.

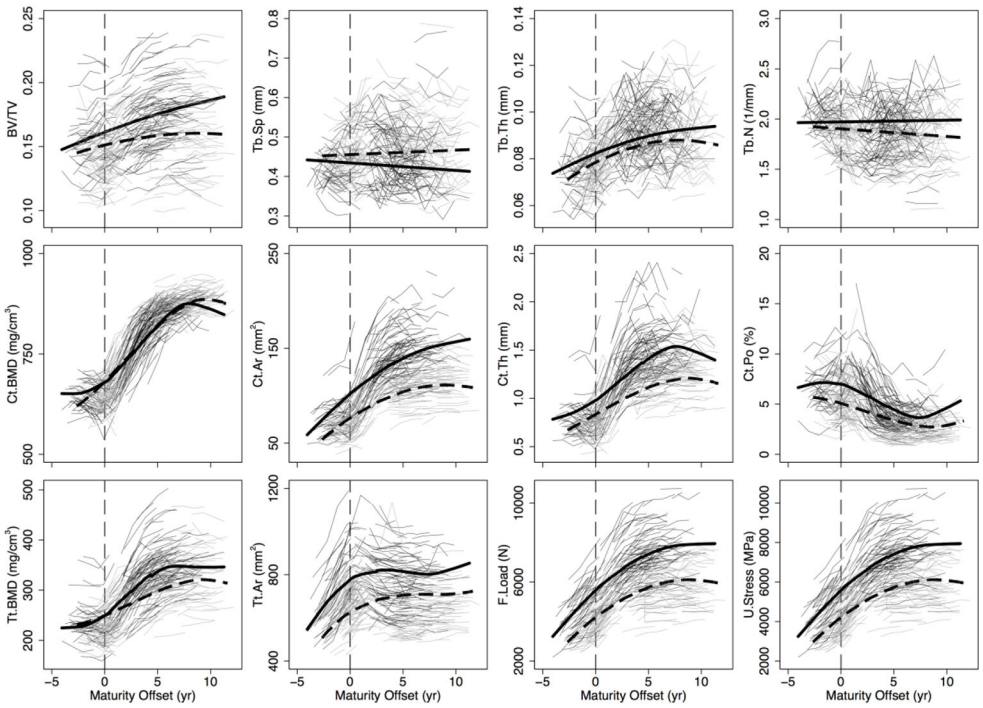

Figure 2.

Distal tibia individual growth curves for boys (thin, black lines) and girls (thin, light grey lines) and the polynomial mixed model growth curves for boys (thick, black solid line) and girls (thick, black dashed line) for trabecular bone volume fraction (BV/TV), separation (Tb.Sp), thickness (Tb.Th) and number (Tb.N), cortical BMD (Ct.BMD), area (Ct.Ar), thickness (Ct.Th) and porosity (Ct.Po), and total BMD (Tt.BMD), area (Tt.Ar), failure load (F.Load), and ultimate stress (U.Stress). The vertical line indicates maturity offset (years from age at peak height velocity) of 0.

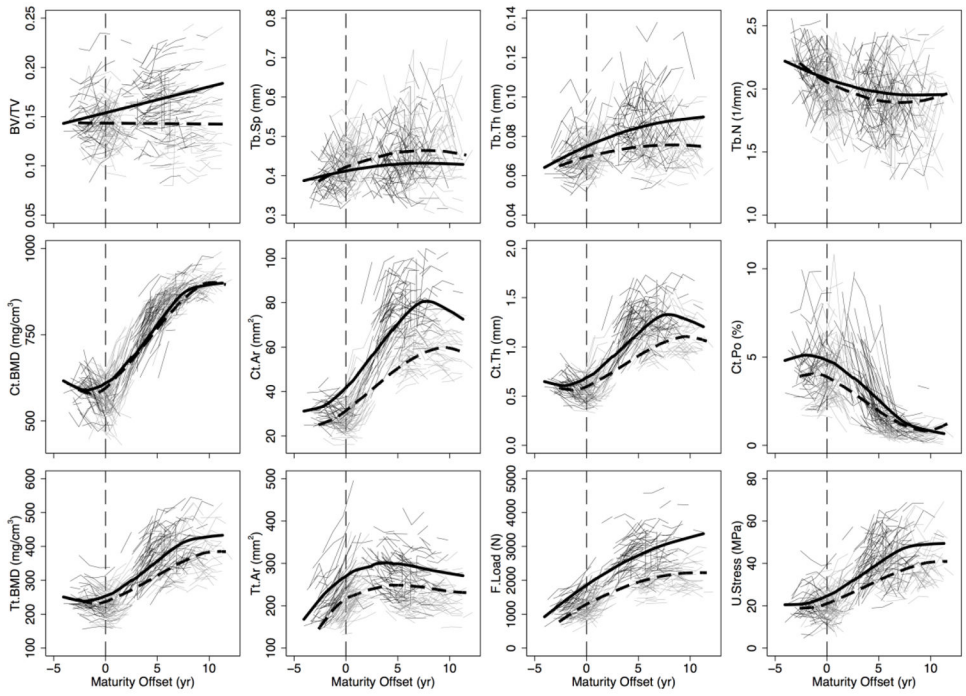

Figure 3.

Distal radius individual growth curves for boys (thin, black lines) and girls (thin, light grey lines) and the polynomial mixed model growth curves for boys (thick, black solid line) and girls (thick, black dashed line) for trabecular bone volume fraction (BV/TV), separation (Tb.Sp), thickness (Tb.Th) and number (Tb.N), cortical BMD (Ct.BMD), area (Ct.Ar), thickness (Ct.Th) and porosity (Ct.Po), and total BMD (Tt.BMD), area (Tt.Ar), failure load (F.Load), and ultimate stress (U.Stress). The vertical line indicates maturity offset (years from age at peak height velocity) of 0.

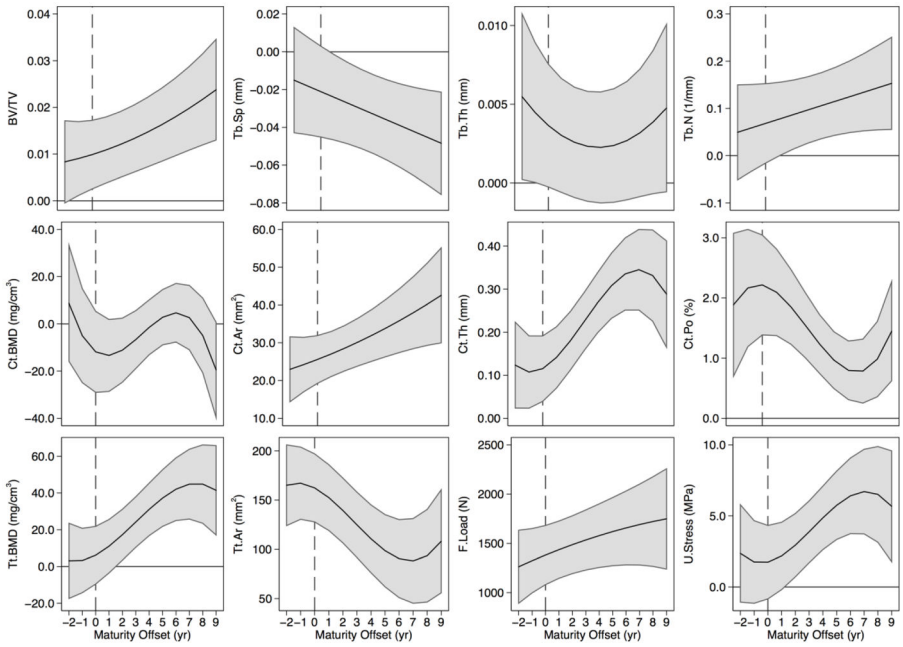

Figure 4.

Sex differences in distal tibia trabecular bone volume fraction (BV/TV), separation (Tb.Sp), thickness (Tb.Th) and number (Tb.N), cortical BMD (Ct.BMD), area (Ct.Ar), thickness (Ct.Th) and porosity (Ct.Po), and total BMD (Tt.BMD), area (Tt.Ar), failure load (F.Load), and ultimate stress (U.Stress) across maturity. The solid black line represents the mean predicted sex difference (boys - girls) accompanied by a shaded 95% confidence interval, correcting for multiple comparisons using a Bonferroni adjustment. Estimates above 0 indicate significantly greater values in boys, while estimates below zero indicate significantly greater values in girls. Confidence intervals that cross 0 indicate non-significant sex differences. The vertical line indicates maturity offset (years from age at peak height velocity) of 0.

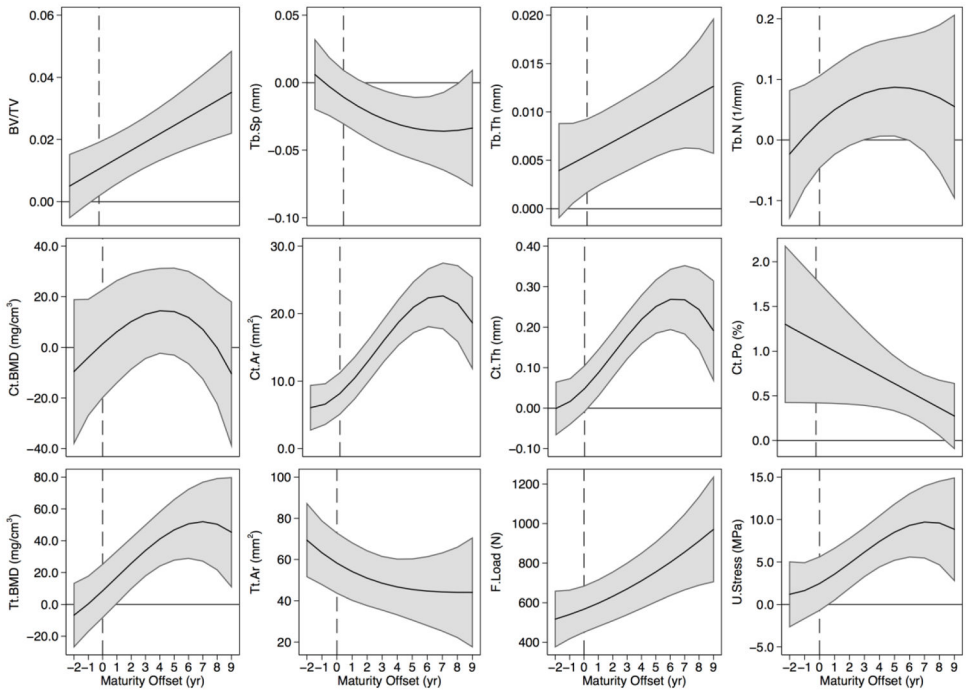

Figure 5.

Sex differences in distal radius trabecular bone volume fraction (BV/TV), separation (Tb.Sp), thickness (Tb.Th) and number (Tb.N), cortical BMD (Ct.BMD), area (Ct.Ar), thickness (Ct.Th) and porosity (Ct.Po), and total BMD (Tt.BMD), area (Tt.Ar), failure load (F.Load), and ultimate stress (U.Stress) across maturity. The solid black line represents the mean predicted sex difference (boys - girls) accompanied by a shaded 95% confidence interval, correcting for multiple comparisons using a Bonferroni adjustment. Estimates above 0 indicate significantly greater values in boys, while estimates below zero indicate significantly greater values in girls. Confidence intervals that cross 0 indicate non significant sex differences. The vertical line indicates maturity offset (years from age at peak height velocity) of 0.

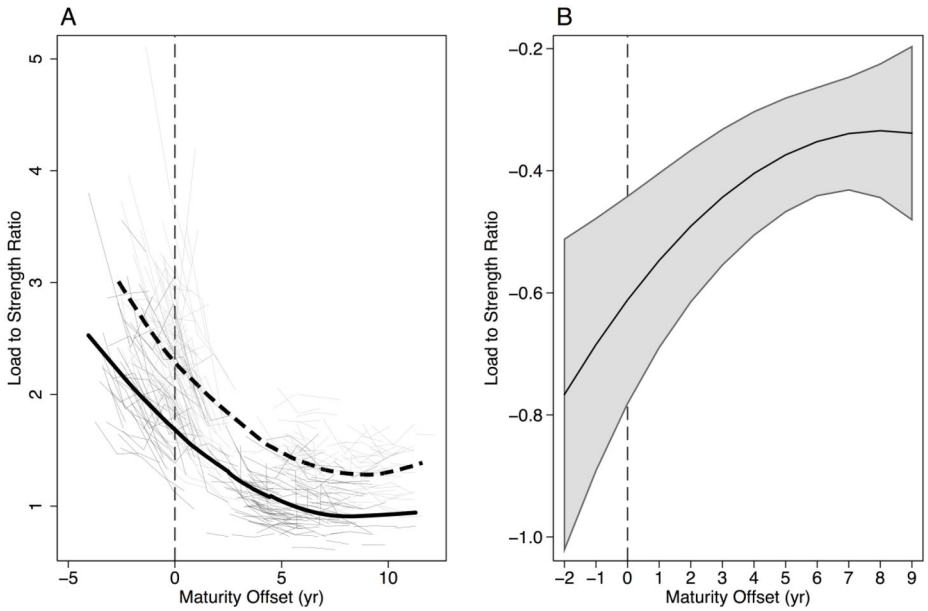

Figure 6.

Load to strength ratio at the distal radius. (A) displays individual data and predicted growth curves for boys (thin black lines and thick black line) and girls (thin grey lines and thick dashed line). (B) displays predicted sex differences (boys-girls) across maturity with 95% confidence intervals, correcting for multiple comparisons using a Bonferroni adjustment. Estimates above 0 indicate significantly greater values in boys, while estimates below zero indicate significantly greater values in girls. Confidence intervals that cross 0 indicate non significant sex differences.

Table 1

Overview of study participants that comprise the Healthy Bones Study III

Cohort	N (sex; ethnicity)	Years of data collection (HR-pQCT assessment)	Study Objective
Healthy Bones Study and Bounce at the Bell[20–23]	N=436 (50% boys; 45% Asian, 44% white, 11% other)	1999–2011 (2008–2011)	Examine the effect of a 20-month cluster-randomized school-based exercise intervention on bone mass
Action Schools! BC[24]	N=515 (50% boys; 55% Asian, 32% white, 13% other)	2003–2011 (2008–2011)	Examine the effect of a 16-month cluster-randomized school-based physical activity intervention on bone mass and strength
New Cohort[4]	N=120 (33% boys; 47% Asian, 44% white, 9% other)	2009–2012 (2009–2012)	Prospective cohort to evaluate changes in bone microarchitecture and strength during the growing years

Table 2

Characteristics of boys and girls at first HR-pQCT measurement

	Boys (n=184)			Girls (n=209)		
	Mean (SD)	**Min**	**Max**	**Mean (SD)**	**Min**	**Max**
Age (yrs)	15.1 (2.6)	9.5	19.8	14.5 (3.4)	9.5	20.3
No. Asian/white/other	82/83/19	-	-	97/92/20	-	-
No. Tanner 1/2/3/4/5	20/14/11/63/75	-	-	31/37/33/58/50	-	-
Maturity (yrs)	3.3 (3.2)	−4.1	11.3	4.3 (3.8)	−2.6	12.2
Height (cm)	167.1 (14.3)	129.7	192.2	155.5 (11.6)	130.0	181.6
Weight (kg)	60.8 (17.3)	27.8	127.3	50.1 (14.1)	22.2	95.9
Sitting height (cm)	88.0 (7.3)	67.2	102.4	83.1 (6.5)	68.6	95.0
Tibial length (mm)	403 (37)	306	482	370 (30)	300	444
Ulnar length (mm)	274 (28)	204	333	246 (21)	196	293
Distal Tibia						
Tb.N (1/mm)	1.90 (0.27)	1.18	2.41	1.81 (0.26)	1.10	2.55
Tb.Th (mm)	0.088 (0.014)	0.055	0.122	0.086 (0.014)	0.056	0.127
Tb.Sp (mm)	0.450 (0.076)	0.326	0.742	0.477 (0.076)	0.320	0.788
BV/TV	0.165 (0.025)	0.108	0.235	0.154 (0.025)	0.093	0.236
Ct.Th (mm)	1.20 (0.37)	0.55	2.35	1.03 (0.31)	0.42	2.01
Ct.Po (%)	5.6 (2.4)	1.6	17.0	3.8 (2.1)	0.7	10.4
Ct.BMD (mg/cm^3)	748.7 (88.5)	577.5	925.3	773.8 (112.6)	552.9	938.1
Tt.BMD (mg/cm^3)	294.4 (59.6)	167.8	441.6	281.7 (60.3)	165.4	466.9
Ct.Ar (mm^2)	119.0 (36.4)	49.4	231.4	92.8 (27.3)	38.2	162.7
Tt.Ar (mm^2)	749.9 (133.2)	454.6	1127.8	624.9 (90.5)	426.9	943.3
F.Load (N)	6212.5 (1683.0)	2185	10700	4912.8 (1317.5)	2434	8425
U.Stress (MPa)	34.3 (9.9)	10.8	55.9	31.7 (9.7)	13.2	60.3
Distal Radius[a]						
Tb.N (1/mm)	1.98 (0.26)	1.28	2.56	1.97 (0.26)	1.37	2.48
Tb.Th (mm)	0.080 (0.015)	0.050	0.136	0.072 (0.010)	0.053	0.120
Tb.Sp (mm)	0.433 (0.070)	0.316	0.689	0.446 (0.073)	0.315	0.673
BV/TV	0.158 (0.030)	0.082	0.246	0.141 (0.026)	0.075	0.237

	Boys (n=184)			Girls (n=209)		
	Mean (SD)	**Min**	**Max**	**Mean (SD)**	**Min**	**Max**
Ct.Th (mm)	1.02 (0.32)	0.40	1.81	0.87 (0.28)	0.41	1.62
Ct.Po (%)	3.4 (2.1)	0.4	11.2	2.4 (1.9)	0.1	9.8
Ct.BMD (mg/cm^3)	729.9 (109.7)	485.5	934.6	735.3 (138.8)	446.3	966.6
Tt.BMD (mg/cm^3)	326.3 (81.8)	155.7	558.9	305.4 (77.9)	167.1	498.9
Ct.Ar (mm^2)	60.7 (21.3)	24.1	104.4	45.1 (16.7)	18.7	92.5
Tt.Ar (mm^2)	262.7 (59.6)	142.8	431.1	206.3 (36.8)	128.7	317.8
F.Load (N)	2295.3 (851.6)	628.5	4576.0	1588.1 (571.1)	477.0	3103.0
U.Stress (MPa)	34.9 (13.5)	4.7	67.4	29.5 (11.4)	6.1	59.9
Load-to-strength Ratio	1.39 (0.62)	0.63	3.80	1.89 (0.73)	0.90	5.11

[a]Sample size for radius parameters: boys (n=166), girls (n=185)

Maturity is estimated as years from age at peak height velocity (APHV)

SD, standard deviation; Tb.N, trabecular number; Tb.Th, trabecular thickness; Tb.Sp, trabecular separation; BV/TV, trabecular bone volume to total volume fraction; Ct.Th, cortical thickness; Ct.Po, cortical porosity, Ct.BMD, cortical bone mineral density; Tt.BMD, total bone mineral density; Ct.Ar, cortical area; Tt.Ar, total area; F.Load, failure load; U.Stress, ultimate stress.

Table 3

Number of HR-pQCT measurements by sex, site and biological age

	Tibia		Radius	
Biological Age	**Boys**	**Girls**	**Boys**	**Girls**
−4	3	-	3	-
−3	22	3	22	3
−2	36	19	35	18
−1	37	55	34	54
0	31	69	26	69
1	31	67	15	66
2	59	33	19	26
3	65	21	44	11
4	79	39	52	10
5	76	61	58	33
6	68	57	50	44
7	43	63	38	42
8	28	64	25	40
9	12	38	12	35
10	5	34	5	33
11	1	19	1	19
12	-	2	-	2
Total	596	644	439	505

Table 4

Estimates of model intercepts for the effects of maturity, sex and ethnicity as predictors of bone parameters at the distal tibia at age at peak height velocity. Numbers in brackets are the standard error of the parameter estimate. Bold values are p<0.05.

	Intercept (γ_{00})	Maturity (γ_{10})	Maturity^2 (γ_{20})	Maturity^3 (γ_{30})	Boys (γ_{01})	Boys by Maturity (γ_{11})	Boys by Maturity^2 (γ_{21})	Boys by Maturity^3 (γ_{31})	Ethnicity (γ_{02})	
									white	other
Tb.N (1/mm)	**1.78 (0.02)**	**−0.01 (0.003)**	-	-	**0.07 (0.04)**	**0.01 (0.004)**	-	-	**0.12 (0.03)**	0.05 (0.04)
Tb.Th (mm)	**0.082 (0.001)**	**0.0026 (0.0003)**	**−0.0002 (0.00002)**	-	**0.004 (0.001)**	**−0.002 (0.0004)**	**−0.0001 (0.00004)**	-	**−0.004 (0.001)**	−0.002 (0.002)
Tb.Sp (mm)	**0.489 (0.007)**	0.001 (0.001)	-	-	**−0.003 (0.001)**	**−0.003 (0.001)**	-	-	**−0.034 (0.008)**	−0.013 (0.013)
BV/TV	**0.147 (0.002)**	**0.002 (0.0003)**	**−0.0001 (0.00003)**	-	**0.010 (0.003)**	**0.002 (0.001)**	0.0001 (0.0001)	-	0.005 (0.003)	0.003 (0.004)
Ct.Th (mm)	**0.84 (0.02)**	**0.07 (0.01)**	0.001 (0.001)	**−0.004 (0.001)**	**0.12 (0.003)**	**0.02 (0.01)**	**0.01 (0.002)**	**−0.001 (0.0001)**	−0.01 (0.02)	**0.10 (0.02)**
Ct.Po (%)	**4.9 (0.2)**	**−0.3 (0.1)**	**−0.1 (0.01)**	**0.01 (0.001)**	**2.2 (0.3)**	−0.1 (0.1)	**−0.1 (0.02)**	**0.01 (0.002)**	0.3 (0.2)	−0.1 (0.3)
Ct.BMD (mg/cm^3)	**679.9 (4.6)**	**25.7 (1.4)**	**2.3 (0.3)**	**−0.3 (0.02)**	**−11.8 (6.0)**	**−3.9 (1.8)**	**2.7 (0.4)**	**−0.3 (0.04)**	−4.1 (3.9)	**16.2 (4.6)**
Tt.BMD (mg/cm^3)	**245.7 (4.5)**	**8.1 (0.9)**	**1.2 (0.2)**	**−0.1 (0.01)**	6.1 (5.5)	**4.0 (1.3)**	**1.0 (0.3)**	**−0.1 (0.02)**	1.1 (4.9)	15.8 (8.3)
Ct.Ar (mm^2)	**74.3 (1.9)**	**8.3 (0.4)**	**−0.5 (0.04)**	-	**25.6 (2.2)**	**1.4 (0.6)**	0.1 (0.1)	-	3.5 (2.2)	**10.7 (3.7)**
Tt.Ar (mm^2)	**575.9 (10.3)**	**39.4 (1.8)**	**−6.7 (0.5)**	**0.3 (0.03)**	**162.3 (12.1)**	**−7.6 (2.5)**	**−2.5 (0.6)**	**0.3 (0.1)**	**66.4 (11.8)**	27.8 (19.7)
F.Load (N)	**3938.6 (90.2)**	**485.6 (15.8)**	**−27.8 (1.4)**	-	**1381.8 (104.8)**	**56.0 (22.7)**	−1.7(2.3)	-	**346.8 (105.7)**	**484.2 (177.0)**
U.Stress (MPa)	**26.8 (0.7)**	**1.9 (0.2)**	0.004 (0.039)	**−0.01 (0.003)**	1.7 (0.9)	0.2 (0.2)	**0.2 (0.1)**	**−0.02 (0.004)**	−0.4 (0.8)	**2.6 (1.3)**

Maturity is estimated as years from age at peak height velocity

Tb.N, trabecular number; Tb.Th, trabecular thickness; Tb.Sp, trabecular separation; BV/TV, trabecular bone volume to total volume fraction; Ct.Th, cortical thickness; Ct.Po, cortical porosity; Ct.BMD, cortical bone mineral density; Tt.BMD, total bone mineral density; Ct.Ar, cortical area; Tt.Ar, total area; F.Load, failure load; U.Stress, ultimate stress.

Table 5

Estimates of model intercepts for the effects of maturity, sex and ethnicity as predictors of bone parameters at the distal radius at age at peak height velocity. Numbers in brackets are the standard error of the parameter estimate. Bold values are p<0.05.

	Intercept (γ_{00})	Maturity (γ_{10})	Maturity^2 (γ_{20})	Maturity^3 (γ_{30})	Boys (γ_{01})	Boys by Maturity (γ_{11})	Boys by Maturity^2 (γ_{21})	Boys by Maturity^3 (γ_{31})	Ethnicity (γ_{02})	
									white	other
Tb.N (1/mm)	**2.00 (0.02)**	**−0.05 (0.01)**	**0.004 (0.001)**	-	0.03 (0.03)	**0.02 (0.01)**	−0.002 (0.001)	-	0.04 (0.02)	0.01 (0.04)
Tb.Th (mm)	**0.070 (0.001)**	**0.002 (0.0003)**	**−0.0001 (0.00003)**	-	**0.005 (0.001)**	**0.001 (0.0004)**	0.000001 (0.0001)	-	−0.0001 (0.0012)	−0.002 (0.002)
Tb.Sp (mm)	**0.437 (0.006)**	**0.013 (0.002)**	**−0.001 (0.0002)**	-	−0.011 (0.007)	**−0.007 (0.002)**	0.001 (0.0003)	-	**−0.013 (0.006)**	0.001 (0.011)
BV/TV	**0.139 (0.003)**	−0.0001 (0.0004)	-	-	**0.010 (0.003)**	**0.003 (0.001)**	-	-	0.004 (0.003)	−0.002 (0.005)
Ct.Th (mm)	**0.63 (0.01)**	**0.03 (0.01)**	**0.02 (0.002)**	**−0.001 (0.0001)**	**0.05 (0.02)**	**0.04 (0.01)**	**0.01 (0.002)**	**−0.001 (0.0002)**	**−0.07 (0.02)**	−0.02 (0.03)
Ct.Po (%)	**3.8 (0.2)**	**−0.2 (0.04)**	**−0.1 (0.01)**	**0.01 (0.001)**	**1.1 (0.2)**	**−0.1 (0.03)**	-	-	**0.3 (0.1)**	0.1 (0.2)
Ct.BMD (mg/cm^3)	**599.2 (5.2)**	**14.4 (2.0)**	**7.9 (0.6)**	**−0.6 (0.04)**	1.4 (7.4)	**5.1 (2.5)**	−0.3 (0.7)	−0.1 (0.1)	**−20.9 (4.8)**	−7.7 (8.0)
Tt.BMD (mg/cm^3)	**244.7 (4.5)**	**4.2 (1.3)**	**4.1 (0.4)**	**−0.3 (0.03)**	8.4 (5.8)	**8.5 (1.7)**	0.3 (0.5)	−0.1 (0.4)	**−16.6 (5.1)**	−10.0 (8.6)
Ct.Ar (mm^2)	**30.5 (0.8)**	**3.2 (0.2)**	**0.5 (0.08)**	**−0.1 (0.01)**	**8.2 (1.1)**	**2.0 (0.3)**	**0.4 (0.1)**	**−0.1 (0.01)**	−0.1 (0.9)	0.7 (1.5)
Tt.Ar (mm^2)	**185.0 (3.9)**	**21.3 (1.1)**	**−3.9 (0.3)**	**0.2 (0.02)**	**58.2 (5.1)**	**−4.5 (1.4)**	0.5 (0.64)	−0.02 (0.04)	**40.1 (4.3)**	**21.3 (7.2)**
F.Load (N)	**1124.7 (34.4)**	**185.8 (8.4)**	**−9.5 (0.9)**	-	**567.3 (40.6)**	**28.7 (11.5)**	1.8 (1.5)	-	**193.0 (41.1)**	113.8 (68.6)
U.Stress (MPa)	**22.1 (0.8)**	**1.4 (0.3)**	**0.3 (0.1)**	**−0.03 (0.01)**	**2.5 (1.1)**	**1.0 (0.3)**	0.1 (0.1)	**−0.02 (0.01)**	**−1.8 (0.9)**	−0.8 (1.5)
Load-to-Strength Ratio	**2.4 (0.04)**	**−0.3 (0.01)**	**0.02 (0.001)**	-	**−0.6 (0.1)**	**0.1 (0.02)**	**−0.004 (0.002)**	-	**−0.1 (0.03)**	−0.1 (0.1)

Maturity is estimated as years from age at peak height velocity

Tb.N, trabecular number; Tb.Th, trabecular thickness; Tb.Sp, trabecular separation; BV/TV, trabecular bone volume to total volume fraction; Ct.Th, cortical thickness; Ct.Po, cortical porosity; Ct.BMD, cortical bone mineral density; Tt.BMD, total bone mineral density; Ct.Ar, cortical area; Tt.Ar, total area; F.Load, failure load; U.Stress, ultimate stress.

J Bone Miner Res. Author manuscript; available in PMC 2018 February 01.